Biomaterials Science

COMMUNICATION

View Article Online
View Journal | View Issue

Cite this: *Biomater. Sci.*, 2019, **7**, 3594

Received 30th January 2019,
Accepted 2nd July 2019

DOI: 10.1039/c9bm00152b

rsc.li/biomaterials-science

Visualizing biofilm by targeting eDNA with long wavelength probe CDr15†

Haw-Young Kwon, ‡[a] Jun-Young Kim,‡[b] Xiao Liu,[a,c] Jung Yeol Lee,[d] Joey Kuok Hoong Yam,[e] Louise Dahl Hultqvist,[f] Wang Xu,[g] Morten Rybtke,[f] Tim Tolker-Nielsen,[f] Wooseok Heo,[c] Jong-Jin Kim,[a] Nam-Young Kang,[d,h] Taiha Joo,[c] Liang Yang,[e] Sung-Jin Park,*[b] Michael Givskov*[e,f] and Young-Tae Chang *[a,b,c]

Detection of the biofilm of bacteria would be a counter strategy to detect hidden bacteria in their camouflage. Through unbiased screening of bacteria biofilm, we discovered a long wavelength probe CDr15 with extracellular DNA as the molecular target. CDr15 revealed a real-time geometric distribution of eDNA in a 3D bacterial colony.

Biofilm is the protecting and camouflaging structure of bacterial colonies. Biofilm is composed of extracellular polymeric substances (EPS) including extracellular proteins, polysaccharides and extracellular DNA (eDNA), to form the 3D structure of a bacterial colony.[1] The composition of EPS or biofilms constantly changes through the regulation of the environment on EPS related genes.[2–6] Therefore, understanding the spatial and temporal characteristics of biofilms requires direct observation of biofilms using fluorescent probes.[7] Detection of eDNA, the primary component for cell-to-cell interconnection, by fluorescent probes helps to clinically diagnose biofilm infection in the early stages.[8] While chronically infected bacteria are often associated with the formation of biofilm, there are very few probes available for direct biofilm detection so far. Commercial NIR dye TO-PRO®-3 was developed to stain the DNA of dead cells,[9] but it cannot be utilized to distinguish eDNA from the DNA of mammalian cell hosts. In our previous study, we established an unbiased screening method for biofilm and developed a yellow fluorescent probe CDy14,[10] which targets the exopolysaccharide, psl, of the biofilm. In this work, we intended to expand the scope of the biofilm probe to longer wavelengths and also to orthogonal targets of biofilm.

In this study, we adopted *P. aeruginosa ΔwspF* with a highly elevated cyclic-di-GMP content (mimicking the biofilm mode of growth) and a *pYhjH* strain with a low intracellular cyclic-di-GMP content[11,12] (representative of the planktonic mode of growth) for unbiased biofilm screening. Around 2000 compounds with long wavelengths (em >700 nm) from the Diversity Oriented Fluorescence Library (DOFL)[13] were screened using a high throughput imaging microscope.[10] The candidate compounds with higher fluorescence contrast in the *ΔwspF* biofilm over *pYhjH* were collected as the primary hits and subjected to further selectivity testing of their target. The screening panel of *P. aeruginosa* is PAO1 (wild type), *ΔwspF*, *pYhjH*, *Δfap (amyloid)*, *Δpsl*, *Δpel* (exopolysaccharide), and *lasIrhll* mutant (Fig. 1A and ESI, Fig. S1†). One unique compound (CDr15, Compound of Designation red 15, Fig. 1B) showed a selective non-staining only in *lasIrhll* mutant unlike PAO1; the *lasIrhll* mutant strain does not secret DNA into the extracellular matrix when it forms biofilms (Fig. 1C).[14] In contrast, CDy14 showed negative staining for the psl mutant (ESI, Fig. S2†). The new probe, CDr15 was from the BODIPY library[15] and showed deep red (733 nm) emission (ESI, Fig. S8, and Table S2†). Due to photoinduced electron transfer (PET), the quantum yield of CDr15 is rather low as 0.009 in DMSO.[16] CDr15 was examined with the two polysaccharide deficient mutants PAO1*Δpel-GFP* and PAO1*Δpsl-GFP*, but the CDr15 signals did not show any significant difference in the staining

[a]*Center for Self-assembly and Complexity, Institute for Basic Science (IBS), Pohang 37673, Republic of Korea. E-mail: ytchang@postech.ac.kr*
[b]*Singapore; Bioimaging Consortium, Agency for Science, Technology and Research, 11 Biopolis Way, # 02-02 Helios, 138667, Singapore. E-mail: park_sung_jin@sbic.a-star.edu.sg*
[c]*Department of Chemistry, Pohang University of Science and Technology (POSTECH), Pohang, Gyeongbuk 37673, Korea*
[d]*New drug discovery Center, Daegu-Gyeongbuk Medivalley Innovation Foundation (DGMIF), 80 Chumbok-ro, Dong-Gu, Daegu, 41061, Republic of Korea*
[e]*Singapore Centre for Environmental Life Sciences Engineering (SCELSE), Nanyang Technological University, 637551, Singapore. E-mail: Mgivskov@sund.ku.dk*
[f]*Costerton Biofilm Center, Department of Immunology and Microbiology, Faculty of Health and Medical Sciences, University of Copenhagen, Blegdamsvej 3B, DK-2200 Copenhagen, Denmark*
[g]*Department of Chemistry & Med Chem Program, Life Sciences Institute, National University of Singapore, 3 Science Drive 3, 117543, Singapore*
[h]*Department of Creative IT Engineering, Pohang University of Science and Technology (POSTECH), Pohang, Gyeongbuk 37673, Korea*

†Electronic supplementary information (ESI) available: Experimental procedures, supplementary tables, figures and spectra. See DOI: 10.1039/c9bm00152b

‡Equal contributing authors.

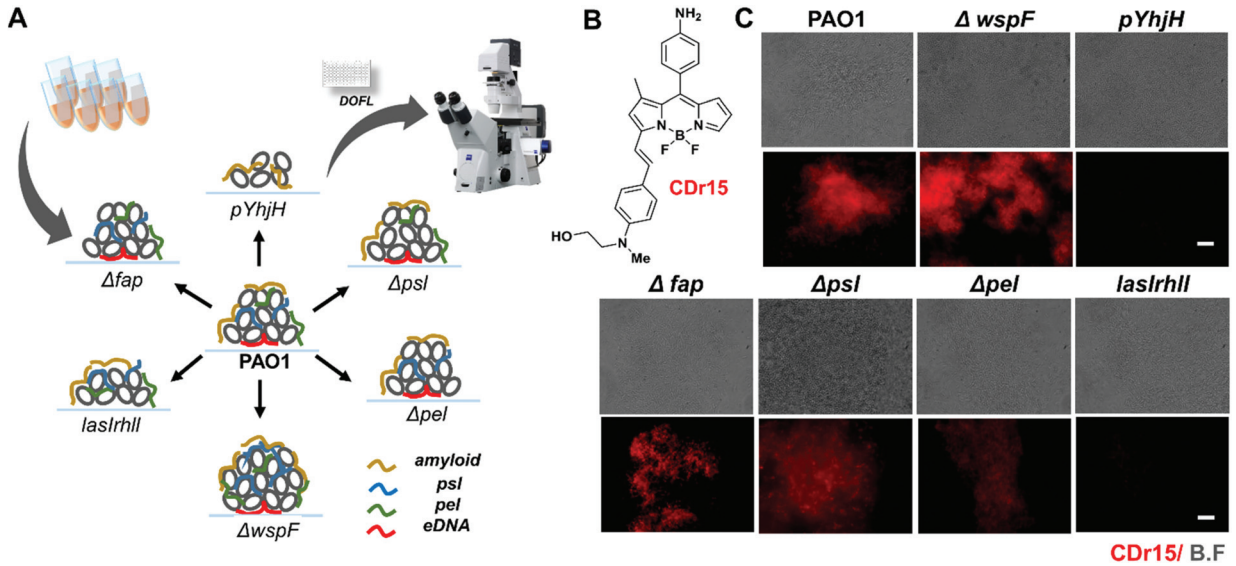

Fig. 1 Development of biofilm selective probes CDr15. (A) Screening scheme for development of the biofilm probe. PAO1, *ΔwspF*, *pYhjH*, *Δpsl*, *Δpel*, *Δfap* and *lasIrhlI* mutant strain were used for screening of eDNA selective probes. The selected compounds were applied to biofilm on a slide as screening and analysed by fluorescent microscopy. (B) Structure of CDr15. (C) The staining CDr15 on the biofilm of the different strains, respectively. Images were taken by fluorescent microscopy. Scale bars, 10 μm.

pattern of the two mutants (ESI, Fig. S3A, and B†). However, CDr15 did not stain the biofilm of *the lasIrhlI* mutant strain, while CDy14 stains the biofilm of the *lasIrhlI* mutant strain (ESI, Fig. S3C†). This result indicates that CDr15 may target the eDNA of the biofilm.

To verify whether eDNA is indeed the binding target of CDr15, we investigated the binding response of CDr15 to nucleic acids and DNA from different sources (bacteria and HEK293) (ESI, Fig. S4A†). We observed a significant dose-dependent increase of CDr15 to DNA (ESI, Fig. S4B†), but a decrease to RNA may be due to aggregation-caused quenching (ACQ) effects (ESI, Fig. S4C†).[17] Both the quantum yield and fluorescence lifetime of CDr15 increased upon DNA binding (ESI, Fig. S4D, and E†). We further tested the staining intensity of CDr15 in PAO1 biofilms after DNase treatment. When DNA in the biofilm matrix was degraded by DNase, the fluorescent intensity of CDr15 was significantly decreased compared to the non-treated biofilms (ESI, Fig. S4F†). Also, the characteristic twitching structure of eDNA[18] was confirmed by CDr15 staining (ESI, Fig. S4G†). The super resolution-SIM and confocal images showed CDr15 signals in the broad region of the extracellular matrix of biofilm, and the signals did not overlap with individual bacteria (GFP expressing live bacteria and membrane staining bacteria ESI, Fig. S4H†). Interestingly, CDr15 did not stain the animal cell nucleus in live, fixed, and fixed and permeablized status (ESI, Fig. S4I, J, and K†). The majority of DNA dyes are cations because of highly negatively charged DNA chains.[19] Therefore, we think that when binding to eDNA, CDr15 is protonated and shows fluorescence enhancement. Compared to eDNA, the crowded environment surrounding the mammalian nucleus makes CDr15 difficult to enter and bind DNA, resulting in dim fluorescence, suggesting the possibility of selective staining of eDNA over infected host cells.

To figure out the CDr15-eDNA binding format, we conducted a competition test between CDr15 and intercalating DNA dye (crystal violet), as well as minor groove-binding DNA dye (Hoechst 33342).[15] CDr15 showed decreasing fluorescence intensity when the concentration of crystal violet increased but no significant intensity change when competing with Hoechst 33342, suggesting that CDr15 binds to eDNA as an intercalator (Fig. S5†).

The localization of the CDr15 staining pattern was further examined by confocal microscopy during the biofilm formation of the 1, 3, and 5-day culture time points. CDr15 staining was found in the basal and core regions of the microcolonies (Fig. 2A), which is well fitted with the previously described localization of eDNA.[20] The vertical section images (Fig. 2B, black box) and the schematic figure (Fig. 2B, lower) shows the spatio-temporal distribution of eDNA in the 3D biofilm microcolonies.

To study the relative localization of eDNA and polysaccharide in the biofilm, CDr15 was co-stained with HHA (Hippeastrum hybrid Lectin, Amaryllis) lection protein, which binds to the Psl polysaccharide of the biofilm.[21] While CDr15 stained the core of the biofilm, HHA-FITC signals occupied the peripheral areas embracing the eDNA region (ESI, Fig. S6†). The relative pattern is well matched to the previously reported eDNA localization,[22] indicating the useful application of CDr15 as an eDNA imaging probe.

Subsequently, we examined the feasibility of CDr15 as a diagnostic tool for detecting biofilms *in vivo*. The chronic infection of bacteria is usually troublesome to detect by conventional culturing techniques, so it would be of great use for detecting biofilm directly from the infection site. Except for culturing, the currently available technique to detect bacteria

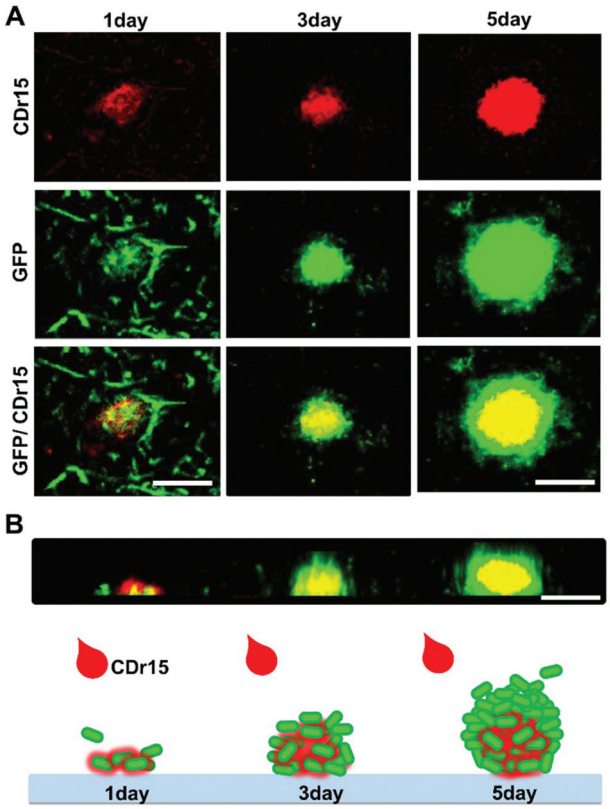

Fig. 2 Localization of CDr15 on biofilm with different development times. (A) Different localization of CDr15 on biofilm showed at different forming times. PAO1-GFP; wild type *P. aeruginosa* was cultured in a chamber slide for 1, 3, and 5 days. CDr15 was applied to biofilm with different development times. The images were taken using a confocal microscope. Scale bars, 10 μm. (B) The CDr15 stain patterns during the biofilm formation were shown in the schematic figure and vertical sectioned images and (black box). Scale bars, 10 μm.

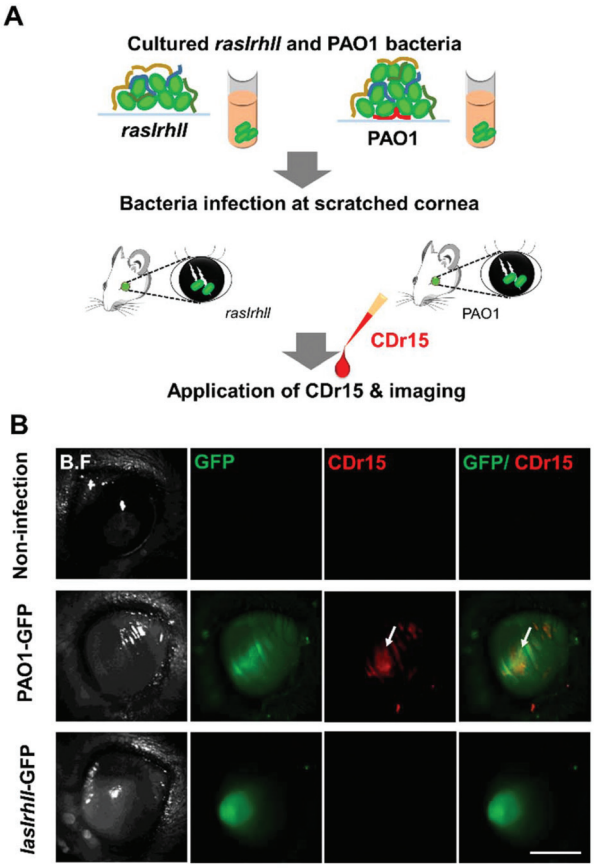

Fig. 3 Detection of biofilm in the infection model with CDr15. (A) Eyes were infected by bacteria (PAO1-GFP, lasIrhII-GFP) through the scratched conical region inducing infection for 1 day. CDr15 (10 μM) was treated on eyes and incubated for 10 minutes. (B) Upper images: non-infection eye, middle images: the infected eye by PAO1-GFP; wild type, bottom images: the infected eyes by lasIrhII-GFP; eDNA-deficient *P. aeruginosa*. All images were observed by a fluorescent stereomicroscope. Scale bars, 2 mm.

is *in situ* hybridization (FISH), a cytogenetic technique using fluorescently labeled complementary DNA or PNA sequences that bind to specific sequences on ribosomal RNA, to judge the presence of bacteria by observing fluorescence.[23] However, the limitation of this technique is that the samples have to be fixed with formaldehyde prior to staining, a methodology which is clearly not ideal for detecting biofilms in clinically relevant conditions. To demonstrate the potential of CDr15 to overcome the current limitation, we chose the mouse corneal infection as the practical H *P. aeruginosa* in contact lens users.[24] Therefore, the corneal infection model, which mimics the natural disease, was generated by scratching cornea in mice with a mini-blade under anesthesia conditions. Subsequently, GFP expressing PAO1 (1–2 μL, 5×10^7–10^8 CFU) was inoculated to the scratched cornea for infections to occur. As controls, PBS and an eDNA deficient *P. aeruginosa* (*lasIrhII-GFP*) strain was inoculated into the scratched corneal regions of different mice. After 1 day of incubation, all the images of the infected corneal regions were examined with CDr15 treatment by a fluorescent stereomicroscope (Fig. 3). When CDr15 (10 μM) was applied to non-infected corneas, no CDr15 background signal was observed (Fig. 3B, upper row). On the other hand, the CDr15 signal was specifically detected only in PAO1 infected cornea (Fig. 3B, middle row), but the fluorescent signals were negative if the infected biofilm was devoid of eDNA (*lasIrhII-GFP*, Fig. 3B, lower row). These results suggested that CDr15 can visualize the biofilm forming regions from the *in vivo* model by selectively targeting the eDNA components. The animal model data along with the long wavelength of the probe, cast the possibility of CDr15 as a diagnostic tool in corneal infection by visualizing biofilm eDNA.

Combination of fluorescent probes with different targets can be of benefit in order to understand biofilm architecture. CDy14 and CDr15 were applied to the 3-day-old biofilm of wild type GFP-expressing *P. aeruginosa* and incubated for 30 min to confirm the different structure imaging in the same biofilm microcolonies (Fig. 4). The CDy14 and CDr15 stain localizations obviously differed as judged from the 3D reconstruction images (Fig. 4A, and ESI, Fig. S7†). CDr15 preferentially showed core and base staining patterns, while CDy14 distinctly

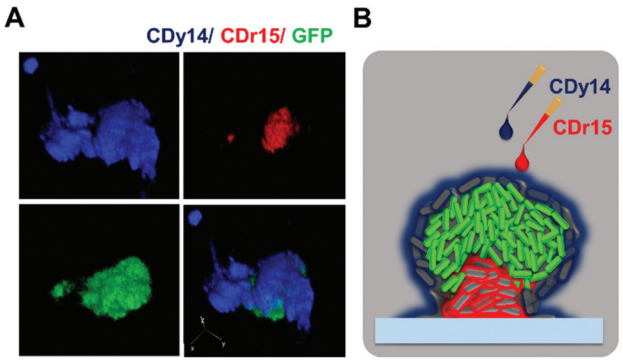

Fig. 4 Double staining of CDy14 and CDr15 on biofilm. PAO1-GFP; wild type *P. aeruginosa* was cultured in the chamber slide for 3 days. Biofilm of PAO1 was stained with CDy14 (blue) and CDr15 (red) for 30 min. (A) 3D images were taken by the confocal microscopy with size 119 μm × 119 μm × 9 μm (*x*, *y* and *z*); calibration *xy*: 0.23 μm, *z*: 0.5 μm. (B) The schematic figure showed the different localization of CDy14 and CDr15 in the microcolony of biofilm.

stained the surface and peripheral areas of the microcolonies. These localization data corroborate that CDy14 and CDr15 target Psl or eDNA,[20] and this is the first experimental demonstration of the co-localization of Psl and eDNA in real-time monitoring as depicted in the schematic Fig. 4B.

Conclusions

In this report, we developed a new fluorescent bioimaging probe CDr15, which targets the extracellular matrix DNA (eDNA) and plays an important role in the construction, maintenance and perpetuation of bacterial biofilms[25,26] in *P. aeruginosa*. Without being influenced by mammalian cells, the relative localization of eDNA and other components in biofilm could be visualized by CDr15. In a corneal infection model, we also successfully demonstrated the feasibility of CDr15 as a diagnostic tool by visualizing *P. aeruginosa* biofilms. Therefore, it is possible to detect bacteria in the early stages by selective eDNA staining of infected host cells in the mode of biofilm. In addition, our developed Psl targeted probe, CDy14, and eDNA targeted probe, CDr15, could be used as biofilm imaging probes for *in vitro* and *in vivo* experiments. Hence, by combining different targeted probes such as CDy11,[27] CDy14 [10] and CDr15, biofilm types can be identified based on the different matrix components. This is of certain guiding significance for the accurate diagnosis and treatment of patients with biofilm infection.

Author contribution

H.Y.K., J.Y.K., L.Y., S.J.P, M.G., and Y.T.C. participated in study conception and designed the experiments. X.L, J.Y.L., and W. X. designed the chemical compounds, performed chemical synthesis, and characterized the compounds. W.S.H and T.H.J. performed and designed the compound life time experiment. H.Y.K., J.Y.K., J.K.H.Y., and N.Y.K. performed experiments including maintaining diverse modified bacterial strains, developing compound stain methods, confocal imaging, super resolution imaging, and double staining imaging. J.Y.K, J.J.K, N.Y.K and S.J.P. performed the *in vivo* animal imaging experiments. H.Y.K., J.Y.K., L.D.H., M.R., T.T., L.Y., S.J.P., M.G., and Y.T.C. analyzed and interpreted data. S.J.P., M.G., and Y.T.C. supervised all experiments. H.Y.K., J.Y.K, T.T., L.Y., S.J.P., M.G. and Y.T.C. wrote the manuscript.

Ethical statement

All animal procedures were performed in accordance with the Guidelines for Care and Use of Laboratory Animals of National University of Singapore (NUS) and approved by the Institutional Animal Care and Use Committee for Biological Resource Center at A*STAR, Singapore.

Conflicts of interest

J.-Y.K., M.G., L.Y., and Y.-T.C. are the inventors of CDy14 for which a patent has been applied.

Notes and references

1 M. E. Davey and G. A. O'toole, *Microbiol. Mol. Biol. Rev.*, 2000, **64**, 847–867.
2 H. M. Dalton, L. K. Poulsen, P. Halasz, M. L. Angles, A. E. Goodman and K. C. Marshall, *J. Bacteriol.*, 1994, **176**, 6900–6906.
3 G. M. Wolfaardt, J. R. Lawrence, R. D. Robarts, S. J. Caldwell and D. E. Caldwell, *Appl. Environ. Microbiol.*, 1994, **60**, 434–446.
4 M. C. M. Van Loosdrecht, *et al.*, *Water Sci. Technol.*, 1995, **32**, 35–43.
5 S. Møller, D. R. Korber, G. M. Wolfaardt, S. Molin and D. E. Caldwell, *Appl. Environ. Microbiol.*, 1997, **63**, 2432–2438.
6 A. T. Nielsen, T. Tolker-Nielsen, K. B. Barken and S. Molin, *Environ. Microbiol.*, 2000, **2**, 59–68.
7 J. Azeredo, N. F. Azevedo, R. Briandet, N. Cerca, T. Coenye, A. R. Costa, *et al.*, *Rev. Microbiol.*, 2016, **3**, 313–351.
8 L. Tang, A. Schramm, T. R. Neu, N. P. Revsbech and R. L. Meyer, *FEMS Microbiol. Ecol.*, 2013, **86**, 394.
9 R. Nakao, S. L. Myint, S. N. Wai and B. E. Uhlin, *Front. Microbiol.*, 2018, **9**, 2605.
10 H. Y. Kwon, J. Y. Kim, J. Y. Lee, J. K. H. Yam, L. D. Hultqvist, W. Xu, M. Rybtke, T. Tolker-Nielsen, J. J. Kim, N. Y. Kang, L. Yang, S. J. Park, M. Givskov and Y. T. Chang, *Chem. Commun.*, 2018, **54**, 11865.
11 S. L. Chua, S. Y. Tan, M. T. Rybtke, Y. Chen, S. A. Rice, S. Kjelleberg, T. Tolker-Nielsen, L. Yang and M. Givskov, *Antimicrob. Agents Chemother.*, 2013, **57**, 2066.

12 L. D. Christensen, V. G. Maria, M. T. Rybtke, H. Wu, W. C. Chiang, M. Alhede, N. Høiby, H. Niels, T. E. Nielsen, M. Givskov and T. T. N. Nielsen, *Infect. Immun.*, 2013, **81**, 2705.
13 S. H. Alamudi and Y. T. Chang, *Chem. Commun.*, 2018, **54**, 13641.
14 H. M. Allesen, K. B. Barken, M. Klausen, J. S. Webb, S. Kjelleberg, S. Molin, M. Givskov and N. T. Tolker, *Mol. Microbiol.*, 2006, **59**, 1114.
15 C. Leong, S. C. Lee, J. Ock, P. See, S. J. Park, F. Ginhoux, S. W. Yun and Y. T. Chang, *Chem. Commun.*, 2014, **50**, 1089.
16 D. Su, J. Oh, S. C. Lee, J. M. Lim, S. Sahu, X. Yu, D. Kim and Y. T. Chang, *Chem. Sci.*, 2014, **5**, 4812.
17 D. Zhai, W. Xu, L. Zhang and Y. T. Chang, *Chem. Soc. Rev.*, 2014, **43**, 2402.
18 S. Wang, X. Liu, H. Liu, L. Zhang, Y. Guo, S. Yu, D. J. Wozniak and L. Z. Ma, *Environ. Microbiol. Rep.*, 2015, **7**, 330.
19 P. Del Castillo, R. W. Horobin, A. Blázquez-Castro and J. C. Stockert, *Biotech. Histochem.*, 2010, **85**, 247.
20 S. Lory, M. Merighi and M. Hyodo, *Nucleic Acids Symp. Ser.*, 2009, **53**, 51.
21 L. Ma, H. Lu, A. Sprinkle, M. R. Parsek and D. J. Wozniak, *J. Bacteriol.*, 2007, **189**, 8353.
22 D. Zhai, Y. Q. Tan, W. Xu and Y. T. Chang, *Chem. Commun.*, 2014, **50**, 2904.
23 C. Almeida, N. F. Azevedo, S. Santos, C. W. Keevil and M. J. Vieira, *PLoS One*, 2011, **29**, e14786.
24 D. M. Robertson and H. D. Cavanagh, *Clin. Ophthalmol.*, 2008, **2**, 907.
25 M. Okshevsky and R. L. Meyer, *Crit. Rev. Microbiol.*, 2015, **41**, 341.
26 C. B. Whitchurch, T. Tolker-Nielsen, P. C. Ragas and J. S. Mattick, *Science*, 2002, **295**, 1487.
27 J. Y. Kim, S. Sahu, Y. H. Yau, X. Wang, S. G. Shochat, P. H. Nielsen, M. S. Dueholm, D. E. Otzen, J. Y. Lee, M. M. Delos Santos, J. K. Yam, N. Y. Kang, S. J. Park, H. Y. Kwon, T. Seviour, L. Yang, M. Givskov and Y. T. Chang, *J. Am. Chem. Soc.*, 2016, **138**, 402.